Vol 14 No 11, November 2005
1009-1963/2005/14(11)/2214-08

Chinese Physics

© 2005 Chin. Phys. Soc.
and IOP Publishing Ltd

Numerical study of the coupling between F_0 with varied numbers of c-subunits and F_1 in an ATP synthase*

Qian Jun(钱 钧), Xie Ping(谢 平),
Dou Shuo-Xing(窦硕星), and Wang Peng-Ye(王鹏业)†

Laboratory of Soft Matter Physics, Beijing National Laboratory for Condensed Matter Physics, Institute of Physics, Chinese Academy of Sciences, Beijing 100080, *China*

(Received 18 March 2005; revised manuscript received 19 August 2005)

ATP synthase is a rotary motor which is composed of two portions: the 'rotor' F_0, consisting of a c-ring, and the 'stator' F_1, consisting of an $\alpha_3\beta_3$ hexamer. In different species, the number of c-subunits which form the c-ring is varied from 10 to 14, whereas the $\alpha_3\beta_3$ hexamer is fixed to be 3-fold symmetrical. We have numerically studied the rotational coupling between F_0 with varied number of c-subunits and F_1. It is found that, for any number of c-subunits, the rotor F_0 advances 3 steps per revolution on average, which is determined by the period of F_1, whereas the exact angular pausing positions are determined by the period of F_0. When the symmetry of the c-ring of F_0 is matched with the 3-fold symmetry of F_1, the three steps have equivalent sizes. If not matched, the three steps become nonequivalent: both the step size and average dwell time are different for these steps.

Keywords: ATP synthase, rotational coupling, numerical simulation
PACC: 3620, 8715B, 8715H, 8715K

1. Introduction

ATP synthase is a universal enzyme in biological energy conversion that is present in the membranes of mitochondria, chloroplasts and bacteria with similar structure and function in different species.[1−6] It synthesizes ATP from ADP and inorganic phosphate (Pi) using the energy of a transmembrane electrochemical gradient of protons (or Na^+ ions). The enzyme is bipartite. Its membrane-embedded F_0-portion transports protons down the electrochemical gradient and generates torque. The peripheral F_1-portion synthesizes ATP at the expense of this mechanical energy.

The general structure of ATP synthase is shown in Fig.1, in which the entire structure is seen arranged as an assembly of 'rotor' and 'stator'. The soluble component F_1 (stator) consists of catalytic sites contained in the $\alpha_3\beta_3$ hexamer, together with subunits a, b_2 and δ. The membrane-spanning component F_0 (rotor) consists of 10–14 c-subunits arranged in a ring and connected to the γ- and ε- subunits that form the central 'shaft'. Proton flow through the channels at the $a-c$ interface generates torque which drives F_0 to rotate. F_1, containing three catalytic sites ($\beta_1\beta_2\beta_3$), produces three ATPs sequentially in one revolution as a three-stepped rotary engine. Each c-subunit translocates one proton, and in one revolution n (the number of the c-subunits) protons are transported across the membrane, which generates a sufficiently large torque to produce three ATPs in F_1.

Interestingly, the number of c-subunits forming the c-ring is not fixed but varies among species. It is believed that n=10–12 in Escherichia coli and n=10, 11 or 14 in other organisms.[4] Hence, there is obviously a rotational mismatch between F_0 and F_1 in many cases. For n=12, the H^+ to ATP stoichiometry is 4. It means that four protons passing through the membrane will lead to the generation of one ATP. In this case, there are four substeps (each through an angle of $2\pi/12$) in a 120° rotation of $\gamma\varepsilon$ relative to F_1. However, for n=10, 11, 14, the H^+/ATP ratio is not an integer (10/3, 11/3, 14/3, respectively). In this case, a key problem exists for the rotational mismatch

*Project supported by the National Natural Science Foundation of China (Grant Nos 60025516 and 10334100).
†E-mail: pywang@aphy.iphy.ac.cn

between the c-ring and F_1 symmetry.

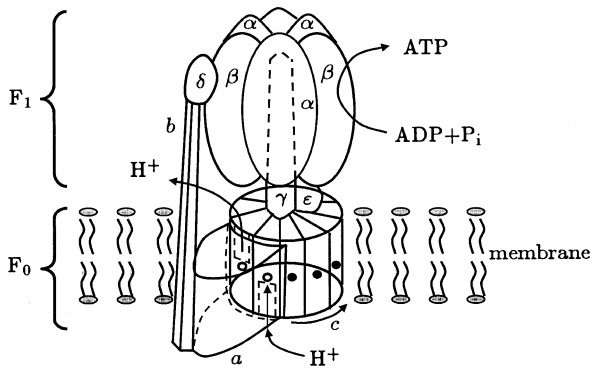


Fig.1. Structure of F_0F_1 ATP synthase. The F_1 portion consists of subunits $\alpha_3\beta_3\gamma\varepsilon\delta$. The F_0 portion consists of subunits ab_2c_n(n=10–14). The proton channels lie at the interface between the a- and c-subunits (dashed lines indicate the putative inlet and outlet channels). Proton flow through the channels develops a torque between the a- and c-subunits. This torque is transmitted to F_1 via the γ shaft and the ε subunit.

In previous studies,[7,8] an elastic strain mechanism was used to interpret the symmetry mismatch between the c-ring and F_1. It is assumed that the energy of each c-subunit movement is stored within the protein until it is sufficient to move $\gamma\varepsilon$ through a 120° rotation with the resulting synthesis of one ATP molecule. However, other researchers argued that the movement of each c-subunit is separately linked to a substep of $\gamma\varepsilon$ rotation and hence to a partial reaction in ATP synthesis.[2,9] Thus the detailed coupling mechanism between F_0 and F_1 is still an open question. In this paper, we neglect the elasticity of the stator and consider the $\gamma\varepsilon$ as an approximately rigid shaft as in some previous studies.[10–12] Using the theoretical model of Ref.[13] for F_0, we study numerically the rotational coupling between F_0 and F_1 in which F_0 has varied number of c-subunits (n=10, 11, 12, 14).

2. Model of the F_0 rotor

The prevailing model for torque generation by proton flow in the F_0 rotor has been proposed in Refs.[13] and [14]. The basic assumptions for this mechanism are: (i) there are two non-collinear access channels for protons from either basic or acid side; (ii) there are two electrostatic constraints: namely, the Asp residue in the middle of the hairpin of the c-subunit which is unprotonated when in contact with the subunit a and protonated when facing the core of the membrane; (iii) there is a Brownian rotary motion of the c-ring relative to the large subunit a. The schematic model for proton transfer and torque generation is shown in Fig.2(a). Proton is allowed to enter the proton carrier (Asp61) of the c-subunit from the acid and basic sides through the two half-channels. There are two negatively charged (unoccupied) rotor Asp61 sites at the rotor-stator interface. The two rotor sites can be either protonated or not. The unprotonated site cannot rotate out of the rotor-stator interface because it would encounter the electrostatic barrier arising from the discontinuity in the dielectric constant between the stator and the membrane. When occupied by a proton, the rotor site can be considered almost neutral and it faces but a small electrostatic barrier when leaving the stator to the membrane. Thus all the rotor sites facing the membrane must be protonated. The positive stator charge (Arg210) is located on the a-subunit offset from the plane of the rotor and interacts electrostatically with the rotor sites. Each proton is first transported to an Asp61 of the c-subunit through a half channel, and then after one revolution of the c-ring, the proton is released to cytoplasm through another half-channel. Owing to the transmembrane proton gradient, the rotor will diffuse preferentially to the right and provide the unidirectional torque for F_1.

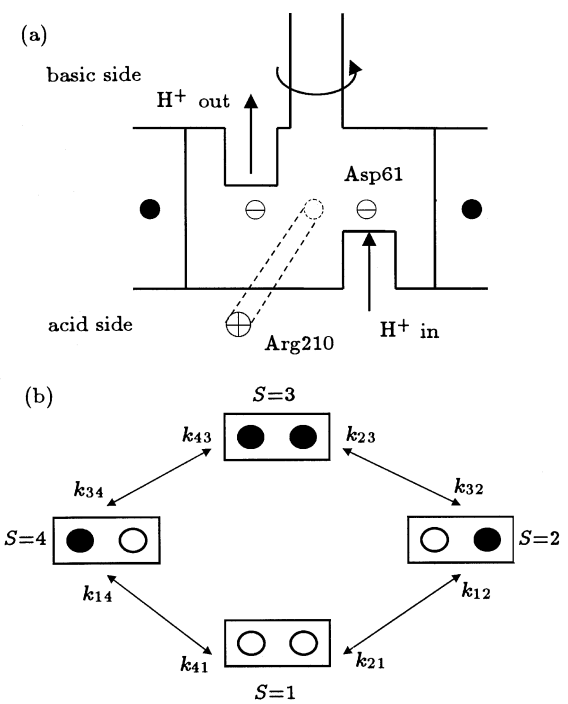


Fig.2. Functional model of F_0. (a) Simple model for proton transfer. The relative locations of the stator and rotor charges and the proton channels are shown. The basic side and acid side are connected by offset 'half-channels'. Arg210 is located on the a-subunit in a plane offset from the plane of the rotor. (b) Markov chain describing the four possible motor states (S=1–4) and their transition rates, k_{ij}. Empty circles, unprotonated Asp61 sites; filled circles, protonated sites.

The rotor-stator interaction depends only on the protonation states of the two rotor Asp61 sites at the rotor-stator interface. As each site can be either protonated or not, there are four possible protonation states of the assembly, as shown in Fig.2(b), denoted by S. In each state the rotor experiences a different torque. Because proton motion is much faster than the rotor's rotation, we can treat the transitions between these states as a Markov chain.[13] Because of the electrostatic interactions between the rotor sites and the stator charge, the transition between the two states depends on the angular position of the rotor, denoted by θ. The evolution of the rotor's chemical state is described by

$$\frac{\mathrm{d}S}{\mathrm{d}t} = k(\theta) \cdot S, \tag{1}$$

where $k(\theta)$ is the matrix of the transition rate between the chemical states.[13,15] (see details in Appendix A)

The rotation of the rotor can be described by the Langevin equation:[16]

$$\zeta\frac{\mathrm{d}\theta}{\mathrm{d}t} = \tau_{\mathrm{Q}}(\theta, S) + \tau_{\mathrm{H}}(\theta, S) - \tau_{\mathrm{L}}(\theta) + \tau_{\mathrm{B}}(t), \quad (S = 1 - 4) \tag{2}$$

where $\frac{\mathrm{d}\theta}{\mathrm{d}t}$ is the angular velocity of the rotor, and ζ the drag coefficient of the rotor. $\tau_{\mathrm{Q}}(\theta, S)$ is the electrostatic torque acting on the rotor from the electrostatic interactions between the stator charge and the rotor sites. The electrostatic interactions are calculated by using a screened Coulomb potential. $\tau_{\mathrm{H}}(\theta, S)$ is the electrostatic barrier that prevents the motion of an unprotonated site into the membrane, with a magnitude of $\sim 45 k_{\mathrm{B}}T$. $\tau_{\mathrm{L}}(\theta)$ is the load torque from F_1, and $\tau_{\mathrm{B}}(t)$ is the Brownian torque from thermal fluctuations. To calculate the rotation of the rotor, Eq.(2) must be solved simultaneously with the Markov process governing the hopping of protons on and off the rotor sites. (see details in Appendix B)

3. Analysis of F_1 motion

The torque generated by the rotation of c-ring is transmitted to F_1 via the γ-shaft. Structural analyses[17−19] have shown that a β subunit with nucleotide-bound state is bent relative to the nucleotide-free state in such a way that its upper portion bend about 30° with respect to the lower part. The eccentric γ-shaft is like a camshaft and its rotation can drive the sequential bending/unbending motions of the β subunits, which correspond to the substrates' binding/release. Several mechanical models of F_1 rotation based on the above mechanism have been proposed.[10−12] According to Boyer's binding change mechanism,[20] a $2\pi/3$ rotation of γ corresponds to a $2\pi/3$ advance in the 'binding changes' states of the three catalytic sites and a $2\pi/3$ advance of the conformational asymmetry of the $\alpha_3\beta_3$ hexamer. Although the detailed enzymatic mechanism for F_1 has not been determined so far, we can simply describe the synthesis of ATP in F_1 as follows: Each $2\pi/3$ rotation of γ causes the unbending of one of the three β subunits, leading to the synthesis and release of one ATP; the other two β subunits are occupied with substrates ADP and Pi to be synthesized, and they are in bending states. In one revolution, the rotation of γ sequentially drives the three β subunits to synthesize and release ATP. Recent study of F_1-motor[21] has shown that a 120° step of F_1 consists of ∼80° and ∼40° substeps. However, in this paper we concentrate on the coupling between the three main 120° steps of F_1 and F_0 motors. So we neglect the 80° and 40° substeps of F_1 for simplicity. Moreover, we assume that the ATP synthase works at saturated [ADP] and [Pi], and thus ignore the time for the binding of ADP and Pi to the β catalytic sites. Therefore, we can treat the load torque from F_1 as a periodic functional form with $2\pi/3$ period. For simplicity, we take it as a cosine form, as shown in Fig.4(a) in next section. In one revolution, the rotor sequentially experiences three load torque peaks, each corresponding to the synthesis and release of one ATP. In each $2\pi/3$ period, the work required to resist the load torque is $25k_{\mathrm{B}}T$, which corresponds to the free energy required for synthesizing one ATP.

4. Results and discussion

The model equations are solved numerically[14] for the cases of different numbers of c-subunits (n=10, 11, 12, 14). The parameter values for F_0 rotor are given in Table 1, which are consistent with those used in Ref.[13]. Figure 3 shows a typical result of the rotation of the rotor with n=10. We see that, on average, the F_0 rotor advances 3 steps per revolution, with one step consisting of 4 substeps (with substep size of $2\pi/10$), and each of the other two steps consisting of 3 substeps. The stepwise movement can be seen more clearly in angular histograms, as shown in Fig.4, which represents the probability distribution of the angular position where the motor stays. (All the angular histograms in this paper were obtained from statistics over a time duration of 0.5 s.) Thus in one

revolution there are totally 10 substeps, and each substep corresponds to the passage of one proton through the motor. From Fig.3, we can also see that backward sub-stepping occasionally occurs.

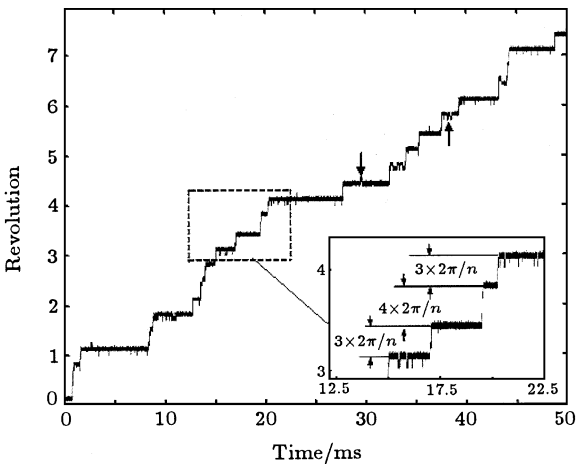


Fig.3. Time evolution of the rotation of the rotor for n=10. Examples of backward and forward substeps are indicated by arrows.

The angular histograms for n=11, 12 and 14 are shown in Figs.5, 6 and 7, respectively. We can see that for most cases the F_0 rotor progresses 3 steps per revolution on average. For n=11, one step consists of 3 substeps with equal substep size, $2\pi/11$, and each of the other two steps consists of 4 substeps. For n=12, each step consists of 4 substeps with equal substep size, $2\pi/12$. For n=14, one step consists of 4 substeps with equal substep size, $2\pi/14$, and each of the other two steps consists of 5 substeps. There are a total of n substeps or n protons passing through the motor per revolution (a 2π rotation).

In order to see the effect of different forms of the load, besides the cosine form, we also use other two forms which are the 'leftward skewed' cosine form and 'rightward skewed' cosine form. They are all taken to be a $2\pi/3$-period function, and the work required to resist the load torque in each period is still $25k_BT$. We give detailed discussions for the results case by case in the following.

In the case of n=10, as shown in Fig.4, first we see that the rotor always stops at the angular positions which are determined by the F_0 period. This can be easily understood from the rotational mechanism of F_0: Under the two electrostatic constraints, the rotor with unprotonated c-subunit facing subunit a always makes a Brownian rotary motion in one period of F_0, and only when a proton hops into the c-subunit can the rotor rotate out of this very F_0 period. Second, as

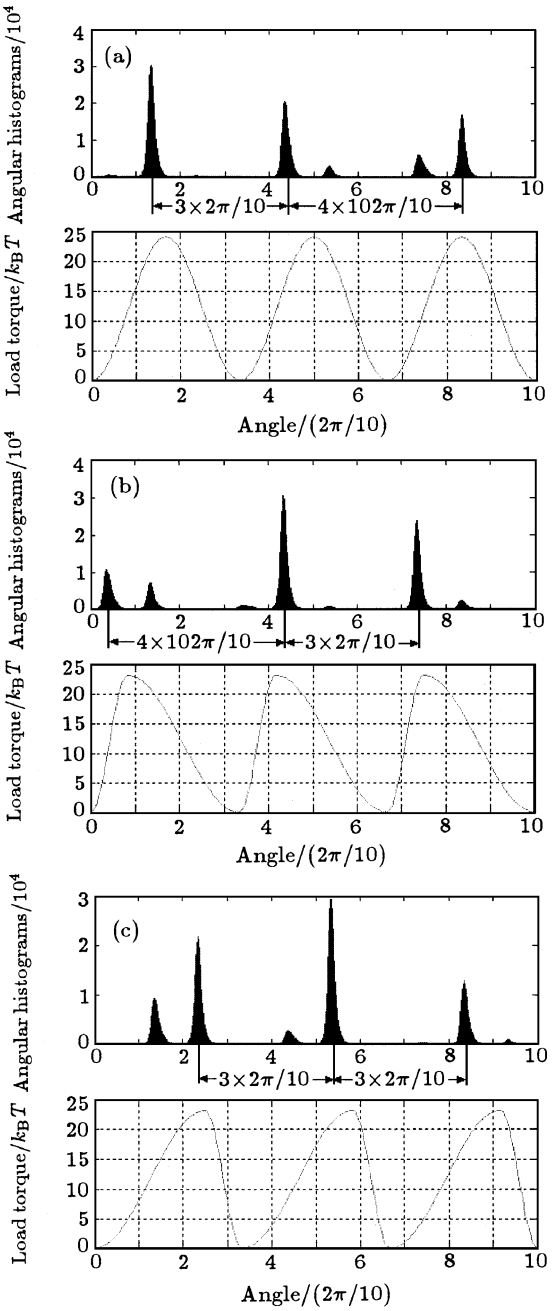


Fig.4. Angular histograms (upper figures) of the rotor with three different forms of load torque (lower figures) for n= 10: (a) the cosine form, (b) leftward skewed cosine form, and (c) rightward skewed cosine form.

anticipated, the rotor has a high probability to stop near the position of the load peak: If the position which is determined from the period of F_0 is coincident with the peak of the torque load from F_1, the rotor has a large probability to stop at the position of the load peak. However, if not coincident, the rotor has a larger probability to stop in the rising phase of the angle-load curve near the peak than in the falling phase. Third, since the number of c-subunits is not matched with the 3-fold symmetrical F_1 catalytic sites, the angle

displaced in one step is not equal to $2\pi/3$. Fourth, by comparing Figs.4(b) and (c) with Fig.4(a) we see that different forms of load torque give similar result and only the relative magnitudes in the angular histogram are different.

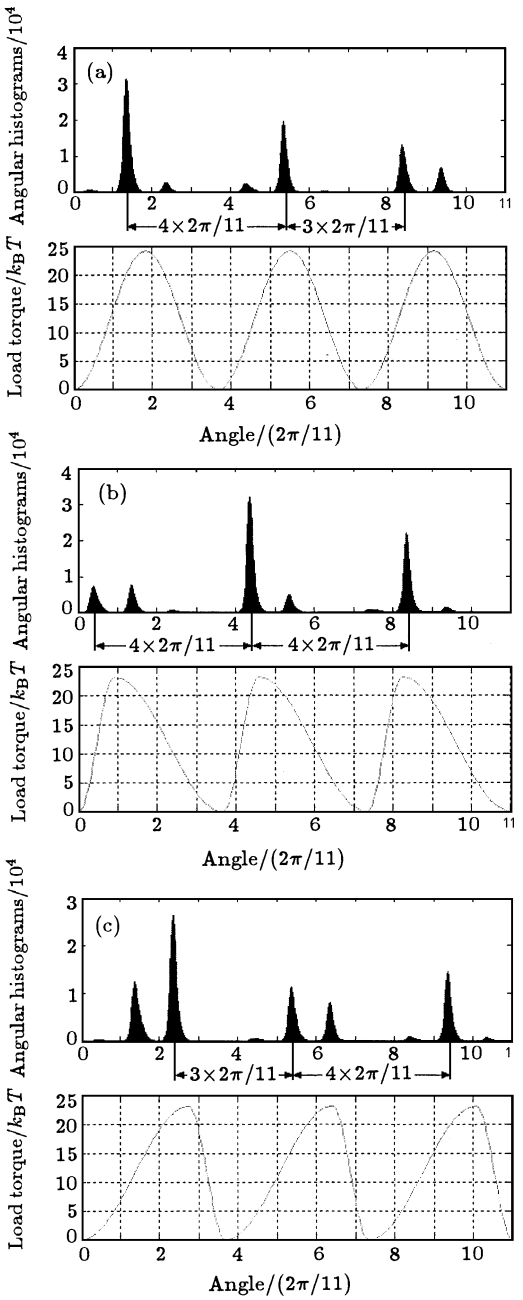


Fig.5. Angular histograms (upper figures) of the rotor with three different forms of load torque (lower figures) for n=11: (a) the cosine form, (b) leftward skewed cosine form, and (c) rightward skewed cosine form.

In the case of n=11, as shown in Fig.5, since the number of c-subunits is still not matched with that of the 3-fold symmetrical F_1 catalytic sites, the characteristics of n=11 are similar to those of n=10 discussed above.

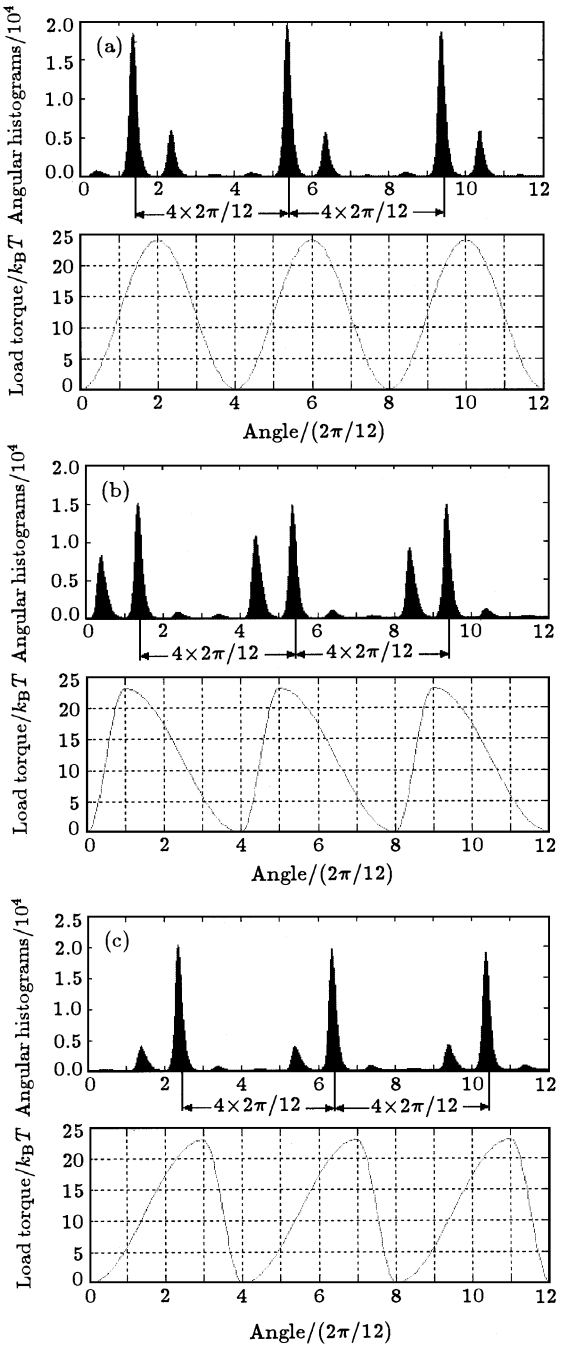


Fig.6. Angular histograms (upper figures) of the rotor with three different forms of load torque (lower figures) for n=12: (a) the cosine form, (b) leftward skewed cosine form, and (c) rightward skewed cosine form.

In the case of n=12, as shown in Fig.6, because the number of c-subunits becomes matched with the 3-fold symmetrical F_1 catalytic sites, the angular histogram becomes symmetric. This means that one load period just corresponds to four periods of F_0, with each step of $2\pi/3$ corresponding to the passage of four protons through the motor. As mentioned before, from Fig.6(a), with the cosine form of the load

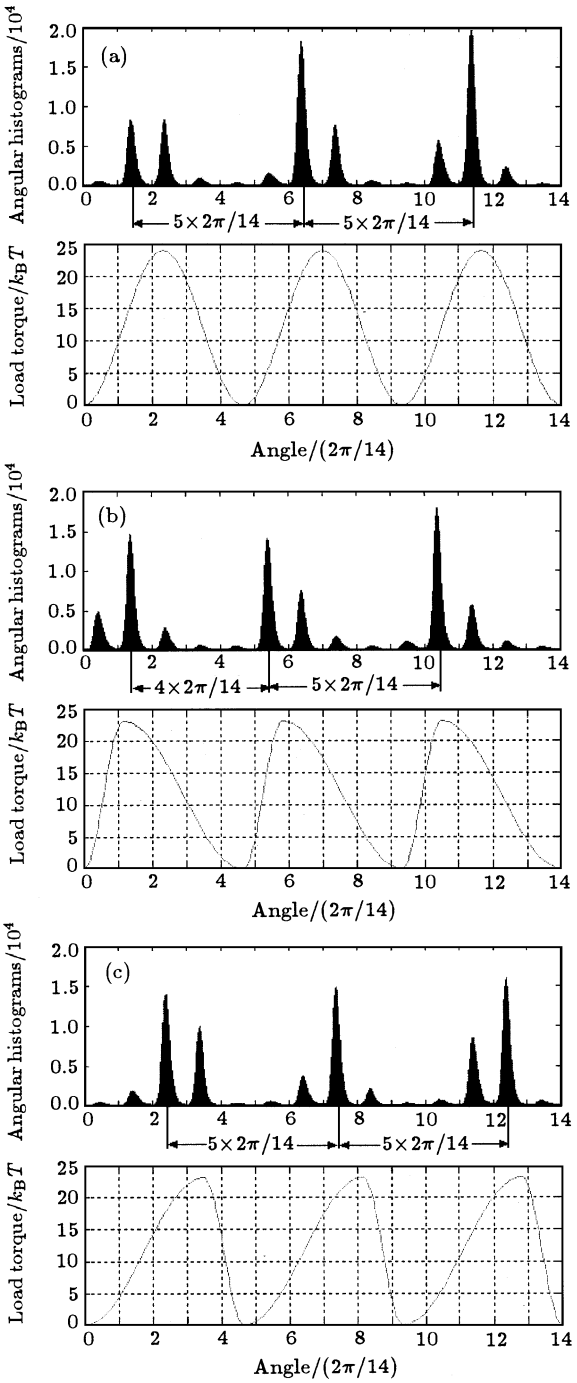


Fig.7. Angular histograms (upper figures) of the rotor with three different forms of load torque (lower figures) for n=14: (a) the cosine form, (b) leftward skewed cosine form, and (c) rightward skewed cosine form.

curve, we see that the rotor has a larger probability to stop in the rising phase near the peak than in the falling phase. In Fig.6(b), with the slope of the rising phase of the load increasing and the slope of the falling phase decreasing, as compared with that of Fig.6(a), the probability for the rotor to stop in the rising phase decreases and the probability to stop in the falling phase increases. In Fig.6(c), with the slope of rising phase of the load decreasing and the slope of the falling phase increasing, as compared with that of Fig.6(a), we see that the probability to stop in the rising phase increases and the probability to stop in the falling phase decreases. Thus we have the following conclusion: The probability for the rotor to stop in the rising phase of the load is higher than in the falling phase; when the slope of the load torque decreases, the probability for the rotor to stop increases.

In the case of n=14, as shown in Fig.7, since the number of c-subunits is not matched with that of the 3-fold symmetrical F_1 catalytic sites, the characteristics become similar to those of n=10, 11. Besides, we note that the angular distribution for each step becomes broadened as the number of F_0 period increases.

Finally, by comparing Fig.6 (matched case) with Figs.4, 5 and 7 (unmatched case), it is interesting to note that, when the F_0 period and the F_1 period are matched, each step takes the same time. However, when the F_0 period and the F_1 period are not matched, the time taken in each step becomes different.

5. Conclusions

We have studied the rotational coupling between stator F_1 and rotor F_0 with varied number of c-subunits (n=10, 11, 12, 14). We found that, for any number of c-subunits, on average, the rotor F_0 advances 3 steps per revolution, which is determined by the period of the stator F_1, whereas the rotor F_0 always stops at the angular positions which are determined by the period of F_0. For the number of c-subunits n=12, which is four times of 3, the probability distribution of the angular position where the motor stays is 3-fold symmetrical, with the angle displaced for each step equal to $2\pi/3$ and each step taking the same time. The passage of four protons through the motor is required for each step. For n=10, 11, 14, which are not integer times of 3, the probability of the angular positions where the motor stays becomes unsymmetrical, with the angle displaced for each step not equal to $2\pi/3$ and the time taken for every step being different. For n=10, one step requires 4 protons and each of the other two steps requires 3 protons; for n=11, one step requires 3 proton and each of the other two steps requires 4 protons; for n=14, one step requires 4 proton and each of the other two steps requires 5 protons.

Appendix A

Transition rates for the rotor sites

The four possible protonation states (s=1, 2, 3, 4) of the two rotor sites at the rotor–stator interface are shown in Fig.2. As protons hop into and out of the channel, the state of the two exposed rotor sites changes. The Markov transition matrix corresponding to the transition diagram in Fig.2 is

$$k = \begin{bmatrix} -\sum_1 & k_{21} & k_{31} & k_{41} \\ k_{12} & -\sum_2 & k_{32} & k_{42} \\ k_{13} & k_{23} & -\sum_3 & k_{43} \\ k_{14} & k_{24} & k_{34} & -\sum_4 \end{bmatrix}, \qquad \text{(A1)}$$

where k_{ij} is the transition rate from the ith state to the jth state; the diagonal entries are given by the sum of all the ways to leave the ith state:

$$\sum_i = \sum_{j \neq i} k_{ij}. \qquad \text{(A2)}$$

The transition rate k_{ij} is zero when the states i and j cannot be connected by the single event of a proton binding onto or dissociating from a rotor site. In matrix (A1), $k_{31} = k_{13} = k_{42} = k_{24} = 0$.

According to Ref.[14], we calculate the proton rate constant as:

$$k_{\rm on} = 0.6{\rm nm}^3 \times 10^{-{\rm pH}} \times 4r \times D_{\rm p}, \qquad \text{(A3)}$$

$$k_{\rm off} = 0.6{\rm nm}^3 \times 10^{-{\rm pK_a}} \times 4r \times D_{\rm p}. \qquad \text{(A4)}$$

Here $k_{\rm on}(k_{\rm off})$ is the proton binding (dissociation) rate. r is the radius of the channel leading to the rotor sites. $D_{\rm p}$ is proton diffusion coefficient. The transition rate k_{ij} is given by adding the potential factor $\exp(\Delta\phi)$ to $k_{\rm on}(k_{\rm off})$. Here $\Delta\phi$ is contributed by the potential drop inside the membrane. The pH of the acidic (basic) reservoir and the pK_a value of the rotor sites in the simulation are listed in Table 1.

Table 1. Parameter values used in the simulation.

Parameter	Value
Proton diffusion coefficient $(D_{\rm p})/({\rm nm}^2{\cdot}{\rm s}^{-1})$	9.3×10^9
Rotary diffusion coefficient of the rotor $(D_{\rm r} = k_{\rm B}T/\zeta)/{\rm s}^{-1}$	2×10^4
Dielectric constant of channel $(\varepsilon_{\rm s})$	10
Dielectric constant of the membrane $(\varepsilon_{\rm m})$	3
Shielding length of channel charges $(1/\lambda)$/nm	1.1
pH of acidic reservoir	7
pH of basic reservoir	8.4
Radius of rotor (R)/nm	5
Membrane potential $(\Delta\psi)$	$5.6k_{\rm B}T$
pK_a of the rotor sites	7.1

Appendix B

The electrostatic interaction between the rotor and stator

The total electrostatic interaction between the rotor and stator consists of two components:

$\phi_{\rm H}(\theta, s)$, is the hydrophobic potential barrier preventing the rotation of the unprotonated rotor sites into the membrane. The energy barrier against rotating an unprotonated Asp61 site into the bilayer depends on the difference in the dielectric constants between the two media: $\Delta G \approx 200\left(\frac{1}{\varepsilon_{\rm membrane}} - \frac{1}{\varepsilon_{\rm stator}}\right)$. Taking $\varepsilon_{\rm membrane} \approx 3$ and $\varepsilon_{\rm stator} \approx 10$, we have $\Delta G \approx 45k_{\rm B}T$.

$\phi_{\rm Q}(\theta, s)$, is the electrostatic interaction between the rotor and the stator charges. The electrostatic interactions are calculated by using a screened Coulomb potential:

$$\tilde{\phi}_{\rm Q} = \frac{q}{4\pi\varepsilon_0}\frac{Q}{\varepsilon_{\rm s} d}\exp(-\lambda d), \qquad \text{(B1)}$$

where d is the distance between the interacting charges q and Q. Here, the stator charge $Q = e$ (elementary charge) and the unoccupied rotor charge $q = -e$. The dielectric constant of the rotor–stator interface is $\varepsilon_{\rm s} = 10$. The screening distance is $1/\lambda$=1.1nm. The electrostatic interaction torque $\tau_{\rm Q}(\theta, s) = -\frac{{\rm d}\phi_{\rm Q}(\theta, s)}{{\rm d}\theta}$.

References

[1] Boyer P D 1999 *Nature* **402** 247

[2] Capaldi R A and Aggeler R 2002 *Trends Biochem. Sci.* **27** 154

[3] Dimroth P, Ballmoos C , Meier T and Kaim G 2003 *Structure* **11** 1469

[4] Weber J and Senior A E 2003 *FEBS Letters* **545** 61

[5] Senior A E and Weber J 2004 *Nature Structural & Molecular Biology* **11** 110

[6] Junge W 2004 *Photosynthesis Research* **80** 197

[7] Cherepanov D A, Mulkidjanian A Y and Junge W 1999 *FEBS Letters* **449** 1

[8] Junge W, Pänke O, Cherepanov D A, Gumbiowski K, Müller M and Engelbrecht S 2001 *FEBS Letters* **504** 152

[9] Senior A E, Nadanaciva S and Weber J 2002 *Biochim. Biophys. Acta* **1553** 188

[10] Wang H and Oster G 1998 *Nature* **396** 279

[11] Sun S X, Wang H and Oster G 2004 *Biophys. J.* **86** 1373

[12] Kinosita K, Adachi K and Itoh H 2004 *Annu. Rev. Biomol. Struct.* **33** 245

[13] Elston T, Wang H and Oster G 1998 *Nature* **391** 510

[14] Junge W, Lill H and Engelbrecht S 1997 *Trends Biochem. Sci.* **22** 420

[15] Grabe M, Wang H and Oster G 2000 *Biophys. J.* **78** 2798

[16] Risken H 1989 *The Fokker–Planck Equation* (New York: Springer-Verlag)

[17] Abrahams J, Leslie A, Lutter R and Walker J 1994 *Nature* **370** 621

[18] Gibbons C, Montgomery M, Leslie A and Walker J 2000 *Nat. Struct. Biol.* **7** 1055

[19] Sun S, Chandler D, Dinner A and Oster G 2003 *Euro. Biophys. J.* **32** 676

[20] Boyer P 1993 *Biochim. Biophys. Acta* **1140** 215

[21] Nishizaka T, Oiwa K, Noji H *et al* 2004 *Nat. Struct. Mol. Biol.* **11** 142